



## Research Article

# Dynamic System State Estimation with a Resilience to Observation Data Anomalies

Andrii Volovyk<sup>1</sup>, Yulia Pyrih<sup>2</sup>, Oksana Urikova<sup>2</sup>, Andriy Masiuk<sup>2</sup>, Bohdan Shubyn<sup>3</sup>,  
Taras Maksymyuk<sup>2\*</sup>

<sup>1</sup> Vinnytsia National Technical University, 95 Khmelnytsky road, Vinnytsia 21000, Ukraine

<sup>2</sup> Lviv Polytechnic National University, 12 Bandery str., Lviv 79013, Ukraine

<sup>3</sup> Silesian University of Technology, 2A Akademick str., Gliwice 44100, Poland

E-mail: voland@vntu.edu.ua

**Received:** 17 April 2023; **Revised:** 1 July 2023; **Accepted:** 9 August 2023

**Abstract:** In practical scenarios, abrupt alterations in system properties can lead to data distortion and random inaccuracies in observation results. These changes often transpire due to malfunctions or failures in individual nodes or subsystems. This paper emphasizes the development of a filter that produces state estimates for control objects capable of withstanding fault actions in the measurement subsystem. To this end, we adjust the observation channel model to accommodate varying accuracy levels, including sudden, abnormal errors. Our filter synthesis leverages Kalman optimal filtering theory methods within the Bayesian framework. This synthesis comprises filtering algorithms that generate the final state vector estimate as a linear combination of model-matched pseudo-Bayesian estimates, weighted by specific coefficients. We justify the existence of these estimates and present an accuracy assessment. Our study particularly emphasizes robust estimators, which are acquired by simplifying either the structure of the optimal estimator or the calculation process of the weighted coefficients. To address the inherent uncertainty of anomalous error probabilities in the observation channel, we suggest an adaptive estimation algorithm grounded in observation outcomes. Simulations were carried out to validate the functionality of the synthesized structures. For instance, we utilized a model depicting an aircraft's movement during an approach, using the MLS system's radio-electronic equipment as an example. We performed a comparative analysis of their accuracy and the associated computational complexity based on the study results.

**Keywords:** adaptation, abnormal errors, Kalman filter, pseudo-Bayesian estimates

**MSC:** 76Z05, 92C10, 92C35

## 1. Introduction

In today's increasingly complex engineering landscape, a broad spectrum of systems and technological processes are being created and employed to tackle a plethora of challenges and requirements. As these systems evolve in sophistication and complexity, the probability of abrupt alterations in their dynamic properties rises. Often, these changes result from the malfunction of specific technical components or subsystems. Unexpected changes like these can lead to data corruption and a de-cline in accuracy, potentially incapacitating the system from performing its intended function. Such aberrations are typically recognized as malfunctions or failures, with their occurrence significantly impacting not only the system's performance and reliability but also the safety and efficiency of the broader engineering operation.

The importance of maintaining seamless system operation is paramount, as system downtimes and failures can result in costly repairs, production delays, and even safety hazards. Hence, it is vital to implement recovery

---

Copyright ©2024 Andrii Volovyk, et al.

DOI: <https://doi.org/10.37256/cm.xxxx>

This is an open-access article distributed under a CC BY license  
(Creative Commons Attribution 4.0 International License)

<https://creativecommons.org/licenses/by/4.0/>

strategies based on the principles of functional and hardware-structural redundancy [1,2]. Leveraging these methodologies, engineers can effectively detect, isolate, and mitigate the impact of failures, thus ensuring the system's sustained performance despite the existence of malfunctions or faults. This proactive approach towards system reliability contributes to the overall efficiency of the engineering operation and enhances the safety and sustainability of the involved processes.

The primary objective of this paper is to develop a robust filter that stays resilient amidst sensory subsystem malfunctions, specifically concerning individual observation abnormal errors. By synthesizing such a filter, the resultant system can maintain its accuracy and stability even when faced with challenges posed by malfunctions, thereby enhancing the overall reliability and integrity of the system in various engineering applications. This ensures the system's ability to operate effectively under a wide array of conditions.

As engineering systems grow increasingly interconnected and interdependent, it becomes crucial to acknowledge the potential cascading effects of malfunctions or failures in one subsystem on the overall system's performance. By addressing these issues at their source and providing robust solutions capable of withstanding real-world application rigors, engineers can develop systems that are not only more reliable and efficient but also more resilient and adaptable to unforeseen challenges.

Apart from developing a robust filter, this paper also explores the underlying principles and methodologies contributing to the successful implementation of functional and hardware-structural redundancy. This includes a comprehensive analysis of existing techniques and the identification of potential areas for improvement and innovation. By building upon the existing body of knowledge and incorporating state-of-the-art research and development, this paper aims to advance the field of system reliability and resilience, laying a robust foundation for future advancements.

The remainder of this paper is structured as follows. Section 2 covers recent related work. Section 3 provides a mathematical formulation of the problem and a description of the proposed approach. Section 4 describes the proposed filter design approach in detail. Section 5 presents simulation results and performance analysis. Finally, Section 6 concludes the article.

## 2. Related work

Over a relatively short period of time, several approaches have been employed to address this problem, with their unique characteristics considered in numerous review papers [3-5,7,9] and monographs [1,2,8] dedicated to certain aspects of fault diagnostics in dynamic systems using analytical redundancy in the form of a priori specified mathematical models. The applied aspects of this problem are partially addressed in works [6,10,11,15–17]. The vast majority of known approaches can be categorized into three main directions that have emerged in recent years. The first direction is based on B. Friedland's work, proposing the concept of expanding the system state vector by introducing a dummy input vector associated with the influence of existing faults and disturbances into its mathematical model. The extended Kalman filter guaranteed the optimality of the problem solution, given the existence of the mathematical model of the artificially introduced unknown input. However, due to the large number of faults and disturbances considered, the dimension of the newly formed extended Kalman filter greatly exceeded that of the nominal system, where faults were not accounted for. To address the challenges of implementing large-dimensional Kalman filters in practice, B. Friedland proposed [18] an approximation of the extended Kalman filter using a two-stage, parallel-acting structure, with independent components. One component estimated faults, while the other estimated the nominal system state vector. The final estimate was formed as a linear combination of weighted individual estimates. However, it was later discovered that the proposed structure only provided a quasi-optimal solution, equivalent to the extended Kalman filter outputs. Extending Friedland's basic provisions to stochastic fault models faced severe practical limitations. Current efforts in this direction focus on finding methods to approximate the extended Kalman filter, combining high accuracy and estimation reliability with practical implementation constraints [11,14,19-22,28].

The second direction assumes the absence of reliable information about the dynamic model of operating faults and their stochastic characteristics. Kitanidis [22] first addressed this problem, developing an algorithm for generating unbiased system state vector estimates by minimizing the covariance matrix trace of estimation errors, subject to linear inequality constraints on system matrices' structure. In [23,24], fault detection and localization were achieved using a geometric approach, generating difference signals with directional properties. An optimal filter with minimum dispersion was synthesized in [25], addressing the accuracy degradation problem inherent in Kitanidis filters. Similar problems were addressed in [21] using a parametric approach.

The third category is based on works that leverage the fundamental principles of adaptive signal processing theory and elements of structural identification [27,28]. This approach frames the problem stochastically, integrating both fault detection and identification methods with those forming the final state vector estimate of a linear discrete system. The proposed method falls into the category of multi-model methods for synthesizing signal

processing systems under a priori uncertainty. We have tailored our method to adapt to the specific tasks of functional diagnostics relating to linear real-time dynamic systems. The essence of the modification is as follows: in the well-established multi-model type methods, the parametric variable typically appears in the deterministic part of the observation equation, assuming the values 0 or 1 with a given probability. This allows for a mathematical description of the random omissions of separate observations. We propose to move the specified parametric variable to the stochastic part of the observation equation, assuming it can assume a set of values with a priori known probabilities from a given range, changing in each computational cycle. This approach enabled us to construct a measurement channel model accounting for varying observation accuracy, including anomalous results. Our innovations have expanded the application scope of the multi-model method for the synthesis of signal processing devices under a priori uncertainty. Additionally, we have paid significant attention to methods for synthesizing quasi-optimal signal processing devices that are computationally simplified and exhibit varying degrees of resilience to the influence of anomalous measurements, while the loss in the estimation process accuracy remains at an acceptable level for practical applications. In instances where quality loss is unacceptable, more accurate but resource-intensive methods of robust nonlinear estimation can be employed. The nuances of using such methods are reflected in recently published works [12–14, 32–35].

### 3. Anomaly-Resilient Solution for Dynamic System State Estimation

#### 3.1 Problem formulation

When the dimension of the observation vector is smaller than the size of the reconstructed state vector, the effectiveness of methods used for synthesizing structures that recover the dynamic system state vector largely depends on the comprehensiveness of a priori information about the mathematical model of the control object and the process generating the output data. In the case of a stochastic formulation of the problem, it is a priori assumed that equations describing their dynamics exist:

$$s(k+1) = \Sigma(k+1, k)s(k) + w(k); \quad s(0) = s_0 \quad (1)$$

$$y(k) = H(k)s(k) + v(k), \quad (2)$$

where  $s(k) \in \mathfrak{R}^n$  – system state vector;  $\Sigma(k+1, k)$  – system transition matrix;  $y(k) \in \mathfrak{R}^m$  – observation vector ( $m < n$ );  $H(k)$  – observation matrix. In addition, it is assumed that  $w(k)$ ,  $v(k)$  are Gaussian uncorrelated random processes that have zero means and correspondingly given covariance matrices  $Q(k)$ ,  $R(k)$ . If information regarding the current state of the observation subsystem does not align with accepted models, is unreliable, or is entirely unavailable, then the synthesis becomes an ill-posed problem [27]. In this case, it would be prudent to modify the problem formulation and shift towards seeking more advanced, functionally extended types of observation result processing. This approach would concurrently address the statistical estimation problem for both the system parameters and the observation channel state. The initial step in this direction should involve correcting the output data generation process model. This revised model would account for the occurrence probability of observations with varying accuracy levels, including abnormal ones.

It is proposed to describe the functionally extended model of the observation subsystem using the equation:

$$y(k) = H(k)s(k) + \varphi(k)v(k); \quad \varphi(k) = 1, \dots, N, \quad (3)$$

where an additional parametric variable  $\varphi(k)$  is introduced that declares the statistical properties of possible faults in the observation channel. The given assumption can be justified by the fact that the optimal structure for reconstructing the system state vector, according to the Kalman method, must consistently strike a balance between the speed of the restoration process and resistance to observational noise. This equilibrium is attained by preserving certain relationships between the covariance matrices of the perturbation noise,  $Q(k)$ , and the observations,  $R(k)$ , regardless of their absolute values. Often referred to as the signal-to-noise ratio in the Kalman filter, the 'useful signal' is represented by the noise process,  $w(k)$ . This balance can be adjusted by, for example, maintaining constant values for  $Q(k)$ , while  $R(k)$  changes according to:

$$R(k) = R_0(k) + \Delta R = R_0(k)[1 + \rho(k)M],$$

where  $R_0(k)$  – the nominal value of the observation noise covariance matrix determined by the regulated accuracy of the observation subsystem;  $\rho$  – the parameter of the uncertainty of the observation channel state;  $M$

– a constant, positive-definite symmetric matrix describing the scale of matrix changes  $\mathbf{R}(k)$ . This rule [22] makes it possible to describe the appearance of different accuracy observations, including abnormal bursts. The influence of the multiplicative component on the final estimation accuracy, in the first approximation, can be considered by introducing an additive component into the nominal model (2) [1], setting  $\varphi(k)=i, i=1,\dots,N; \mathbf{M}=\mathbf{I}_m$ . This proposal can be implemented under terms of the Bayesian methodology or using the principles of adaptive signal processing. In the first case, the result of the synthesis is a set of model-conditional Kalman filters tuned to each of the accepted hypotheses  $\mathbf{R}(k)=\varphi^2(k)\mathbf{R}_0(k)$ . The value of  $N$  can be estimated, for example, from such considerations. As usual, the accuracy of observations is described by the root-mean-square error  $\sigma_0$  however, sometimes accuracy values at the level  $2\sigma_0$  or even  $3\sigma_0$  are given. In the latter case, this means that at least 99% of all observations should be in the band  $\pm 3\sigma_0$ , and those that go beyond these limits give reason to consider them abnormal. Thus, the number of competing hypotheses generally does not exceed three to five, and the abnormal errors probability is determined by the “tails” of the normal distribution located outside the band  $\pm 3\sigma_0$ . If we are only interested in the abnormal errors effect on the resulting measurement accuracy, only two hypotheses can be used. Hypothesis  $\mathcal{H}_1$  corresponds to the situation  $\varphi(k)=1$  – the observation channel is serviceable, and the situation  $\varphi(k)=N(N \gg 1)$  will mean the presence of abnormal bursts (hypothesis  $\mathcal{H}_a$ ). Precisely this variant will be considered in the next section, assuming the use of the reconstructed observation channel model (3).

### 3.2. Synthesis of a Filter Structure Resistant to Abnormal Burst Influences in the Observation Channel

The synthesis of a filter that will be tolerant to the observation subsystem faults will be performed under the terms of the Bayesian methodology using the modified mathematical model of the observation channel.

$$\mathbf{y}(k) = \mathbf{H}(k)\mathbf{s}(k) + \varphi(k)v(k); \quad (4)$$

$$\mathbf{s}(k+1) = \mathbf{Z}(k+1,k)\mathbf{s}(k) + \mathbf{w}(k); \quad \mathbf{s}(0) = \mathbf{s}_0. \quad (5)$$

Information regarding the notation and a priori data has been defined in the previous subsection. The observation channel faults, such as random loss of single measurement observation results or their distortion, in the first approximation, will be considered by an equivalent the observation error covariance matrix increase up to  $N^2\mathbf{R}_0(k)$  for  $N \gg 1$ . It is well known that the optimal estimator that minimizes Bayesian risk is the posterior mean [23].

$$\mathbf{s}_0^* (k) = E\{\mathbf{s}(k)/\mathbf{Y}_1^k\} = \int \mathbf{s}(k)\boldsymbol{\pi}[\mathbf{s}(k)/\mathbf{Y}_1^k]d\mathbf{s}(k) \quad (6)$$

Where,  $E\{\cdot\}$  – conditional expectation;  $\mathbf{Y}_1^k = \{y(1), y(2), \dots, y(k)\}$  – implementation of the observations sequence available at the current time. Given that  $\mathbf{Y}_1^k$  depends on parametric sequence  $\boldsymbol{\varphi}^k = \{\varphi(1), \dots, \varphi(k)\}$ , and processes  $\mathbf{s}(k), y(k)$  are Markovian, it is easy to show that the posterior probability density  $\boldsymbol{\pi}[\mathbf{s}(k)/\mathbf{Y}_1^k]$  can be approximated by the weighted sum  $2^k$  of Gaussian distribution densities for all  $k=0, 1, \dots$ . This is easy to verify if we use the mathematical induction method and the smoothing conditional mean properties. For example, for the first step, the desired distribution density  $\boldsymbol{\pi}[\mathbf{s}(k)/\mathbf{Y}_1^k]$  can be written as the result of averaging of the following form:

$$\boldsymbol{\pi}[\mathbf{s}(k)/\mathbf{Y}_1^k] = E_{\varphi(1)}\{\mathbf{s}(k)/\mathbf{Y}_1^k, \varphi(1)/\mathbf{Y}_1^k\} = \sum_{i=1}^N \boldsymbol{\pi}[\mathbf{s}(k)/\mathbf{Y}_1^k, \varphi(1)/\mathbf{Y}_1^k]p[\varphi(1)=i/\mathbf{Y}_1^k].$$

In the same fashion, we write the representation of the distribution density for the second step:

$$\begin{aligned} \boldsymbol{\pi}[\mathbf{s}(k)/\mathbf{Y}_1^k, \varphi(1)] &= E_{\varphi(2)}\{\mathbf{s}(k)/\mathbf{Y}_1^k, \varphi(2), \varphi(1)/\mathbf{Y}_1^k, \varphi(1)\} \\ &= \sum_{i=1}^N \boldsymbol{\pi}[\mathbf{s}(k)/\mathbf{Y}_1^k, \varphi(2), \varphi(1)]p[\varphi(2)=i/\mathbf{Y}_1^k, \varphi(1)]. \end{aligned}$$

Combining the two steps gives the result:

$$\begin{aligned} \pi[s(k)/Y_1^k] &= E_{\varphi(2)} \left\{ E_{\varphi(1)} \left\{ \left\{ \pi[s(k)/Y_1^k, \varphi(1), \varphi(2)/Y_1^k, \varphi(1)/Y_1^k] \right\} \right\} \right\} \\ &= \sum_{i=1}^N \left\{ \sum_{i=1}^N \pi[s(k)/Y_1^k, \varphi(2), \varphi(1)] p[\varphi(2) = i/Y_1^k, \varphi(1)] \right\} p[\varphi(1) = i/Y_1^k]. \end{aligned}$$

Further application of the mathematical induction method up to the time moment  $k$ , inclusive, allows us to form a branching process, where the posterior distribution density  $\pi[s(k)/Y_1^k]$  can be considered as a weighted sum,  $2^k$  branches-summands:

$$\begin{aligned} \pi[s(k)/Y_1^k] &= E_{\varphi(k)} \left\{ E_{\varphi(k-1), \dots, \varphi(2)} \left\{ E_{\varphi(1)} \left\{ \left\{ \pi[s(k)/Y_1^k, \varphi(k), \dots, \varphi(2), \varphi(1)/Y_1^k, \varphi(k), \dots, \varphi(2)/\dots, \varphi(1)/Y_1^k, \varphi(k)/Y_1^k] \right\} \right\} \right\} \right\} \\ &= \sum_{i=1}^N \dots \sum_{i=1}^N \pi[s(k)/Y_1^k, \varphi(k), \varphi(k-1), \dots, \varphi(2), \varphi(1)] p[\varphi(k), \varphi(k-1), \dots, \varphi(2), \varphi(1)/Y_1^k]. \end{aligned} \quad (7)$$

An analysis of expression (7) shows that the calculation of a strictly optimal estimate  $s^*_o(k/k)$  requires finding a weighted sum of  $2^k$  locally conditional estimates  $s(k)$ . This factor leads to an overload of the processing device with increasing values of  $k$ . From a pragmatic point of view, we assume that the probability distribution density (7) allows a satisfactory approximation for each  $k$  by one equivalent Gaussian distribution. Then, considering the averaging performed, we can find the equivalent parameters  $E\{s(k)/Y_1^{k-1}\} = s^*(\frac{k}{k-1})$ ,  $Cov\{s(k)/Y_1^{k-1}\} = P(\frac{k}{k-1})$  distribution density  $\pi[s(k)/Y_1^{k-1}]$  based on the results from the previous computational cycle, or for  $k = 0$  they must be given a priori. Estimates obtained in this way are not strictly optimal from a mathematical point of view and are called pseudo Bayesian. In contrast to the optimal estimates  $s^*_o(\frac{k}{k})$  we will denote them as  $s^*(\frac{k}{k})$ . As a result,  $\pi[s(k)/Y_1^k]$  allows a simplified form of calculations

$$\pi[s(k)/Y_1^k] = \sum_{i=1}^N \pi[s(k)/Y_1^k, \varphi(k) = i] p[\varphi(k) = i/Y_1^k], \quad (8)$$

and this sum multipliers can be calculated recursively using the Bayes formula and the Markov properties of models (4)–(5). Applying the Bayes rule to the distribution density  $\pi[s(k)/Y_1^k, \varphi(k) = i]$ , we get:

$$\begin{aligned} \pi[s(k)/Y_1^k, \varphi(k) = i] &= \pi[s(k), y(k)/Y_1^{k-1}, \varphi(k) = i] \left\{ \pi[y(k)/Y_1^{k-1}, \varphi(k) = i] \right\}^{-1} = \\ &= \pi[s(k)/Y_1^{k-1}, \varphi(k) = i] \pi[y(k)/Y_1^{k-1}, s(k), \varphi(k) = i] \times \left\{ \sum_{i=1}^N \pi[s(k), y(k)/Y_1^{k-1}, \varphi(k) = i] \right\}^{-1}. \end{aligned} \quad (9)$$

Since the dynamics model (5) doesn't provide for an explicit dependence  $s(k)$  from  $\varphi(k)$ , then  $\pi[s(k)/Y_1^{k-1}, \varphi(k) = i] = \pi[s(k)/Y_1^{k-1}] = N[s^*(\frac{k}{k-1}), \mathcal{P}(\frac{k}{k-1})]$ , where  $N(\bullet)$  – normal distribution symbol. Using model properties (4) gives:

$$\begin{aligned} \pi[y(k)/Y_1^{k-1}, \varphi(k) = i] &= N[\mathbf{H}(k)s^*(\frac{k}{k-1}); \mathbf{H}(k)\mathbf{P}(\frac{k}{k-1})\mathbf{H}^T(k) + \varphi^2(k)\mathbf{R}_0(k)] \\ \pi[y(k)/Y_1^{k-1}, s(k), \varphi(k) = i] &= N[\mathbf{H}(k)s(k), \varphi^2(k)\mathbf{R}_0(k)] \end{aligned} \quad (10)$$

Applying the Bayes formula to probability  $p[\varphi(k) = i/Y_1^k]$  allows us to bring it to the form

$$\begin{aligned} p[\varphi(k) = i/Y_1^k] &= p[y(k), \varphi(k) = i/Y_1^{k-1}] \left\{ p[y(k)/Y_1^{k-1}] \right\}^{-1} \\ &= p[\varphi(k) = i/Y_1^{k-1}] \pi[y(k)/Y_1^{k-1}, \varphi(k) = i] \left\{ \sum_{i=1}^N p[y(k), \varphi(k) = i/Y_1^{k-1}] \right\}^{-1}. \end{aligned}$$

The component  $\pi[y(k)/Y_1^{k-1}, \varphi(k) = i]$  has already been determined, and the second multiplier is found using the properties of conditional probabilities:

$$p[\varphi(k) = i/Y_1^{k-1}] = \sum_{i=1}^N p[\varphi(k-1) = i/Y_1^{k-1}] p[\varphi(k) = i/Y_1^{k-1}, \varphi(k-1) = i], \quad (11)$$

where  $p[\varphi(k-1) = i/Y_1^{k-1}]$  is assumed to be known from the previous calculations cycle and the value  $p[\varphi(k) = i/Y_1^{k-1}, \varphi(k-1) = i] = p[\varphi(k) = i/\varphi(k-1) = i]$  must be specified a priori as an element of the transition probabilities matrix. Obtaining estimates  $s^*(\frac{k}{k})$  is associated with certain difficulties due to the complex system of calculations that shows the above equations. The calculations complexity can be somewhat simplified if we impose additional boundary conditions on the parametric sequence  $\varphi(k)$ , namely, we will consider it uncorrelated,

taking the value  $I, N$  with probabilities given a priori  $p[\varphi(k)=i/Y_1^k]=q_i(k)$ ;  $p[\varphi(k)=N/Y_1^k]=q_N(k)$ . The reason for introducing such a limitation may be the fact that abnormal bursts appear relatively rarely, and the physical factors that generate them act, as a rule, in an independent way. The imposed limitations do not violate the generality of the results obtained, but only apply to the procedures for weight factors calculating  $p[\varphi(k)=i/Y_1^k]$ , which will now have a simplified form:

$$p[\varphi(k)=i/Y_1^k]=q_i(k)\pi[y(k)/Y_1^{k-1},\varphi(k)=i]\left\{\sum_{i=1}^N q_i(k)\pi[y(k)/Y_1^{k-1},\varphi(k)=i]\right\}^{-1}. \quad (12)$$

The structure of the synthesized filter is shown in Fig. 1, and its practical implementation requires the use of a microcomputer. Combining the functions of detecting abnormal errors and estimating the system state vector gives the structure shown in Fig. 1 adaptive features. However, all calculations must be performed at the rate of the observation results receipt. This is due to the fact that the errors correlation matrix, through the posterior probabilities calculation, depends on the current observation results  $y(k)$ :

$$P(k/k)=\left\{P_1(k/k)+[s_1^*(k/k)-s^*(k/k)][s_1^*(k/k)-s^*(k/k)]^T\right\}p[\varphi(k)=1/Y_1^k]+ \left\{P_N(k/k)+[s_N^*(k/k)-s^*(k/k)][s_N^*(k/k)-s^*(k/k)]^T\right\}p[\varphi(k)=N/Y_1^k]. \quad (13)$$

The validity of (13) can be verified if we consider that the estimation accuracy is described by the expression, by definition:

$$E\left\{[s(k)-s^*(k/k)][s(k)-s^*(k/k)]^T/Y_1^k\right\}=\int[s(k)-s_1^*(k/k)][s(k)-s_1^*(k/k)]^T\pi[s(k)/Y_1^k]ds(k),$$

where  $\pi[s(k)/Y_1^k]$  is the weighted sum (8).

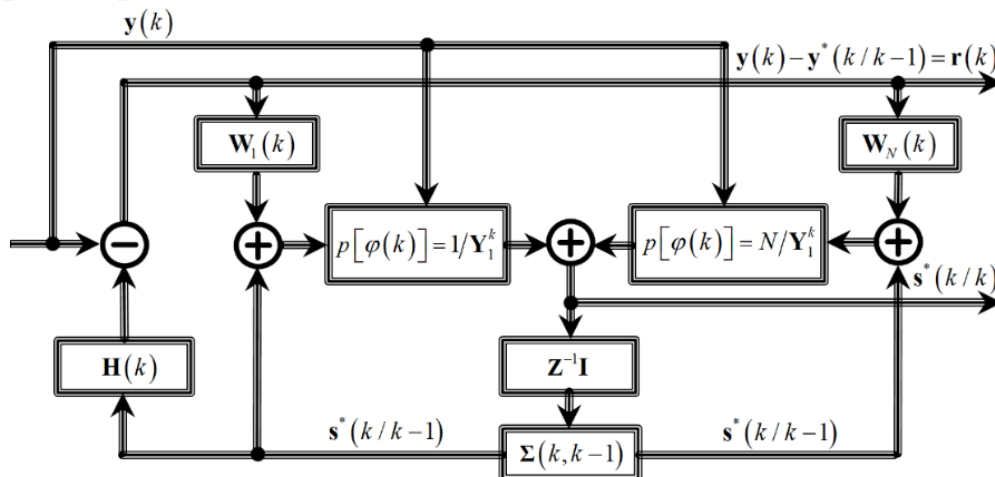


Figure 1. Algorithm for pseudo-Bayesian estimates.

### 3.3. Expanding the Filtering Algorithm for A Priori Uncertainty Probabilities of Fault Occurrence

The observation channel model (4) remains operational even in the case when a priori data of the abnormal errors' probability are unreliable or completely absent. However, in order to remain under terms of the Bayesian methodology, assumptions are made about the uniform law of the value distribution in the range  $\{0 \dots 1\}$ . As in the previous subsection, the estimation of  $s^*(k/k)$  will be calculated as a weighted sum

$$s^*(k/k)=\sum_{i=1}^N s_i^*(k/k)p[\varphi(k)=i/Y_1^k]. \quad (14)$$

The difference is instead of the a priori given value  $q_i(k)$  in expression (12), it is necessary to substitute the average value  $\overline{q_i(k)}$  of this probability. Let us show that it can be calculated by the formula

$$\overline{q_i(k)} = \int_0^1 q_i \pi[q_i / Y_1^k] \pi[y(k) / Y_1^{k-1}, q_i] \{ \pi[y(k) / Y_1^{k-1}] \}^{-1} dq_i. \quad (15)$$

To do this, we present the posterior probability  $p[\varphi(k) = 1 / Y_1^k]$  as

$$p[\varphi(k) = 1 / Y_1^k] = \int_0^1 \pi[\varphi(k) = 1, q_i / Y_1^k] dq_i = \int_0^1 \pi[q_i / Y_1^k] p[\varphi(k) = 1 / Y_1^k, q_i] dq_i. \quad (16)$$

The result of applying the Bayes formula to  $\pi[q_i / Y_1^k]$  gives the result:

$$\pi[q_i / Y_1^k] = \pi[q_i / Y_1^{k-1}] \pi[y(k) / Y_1^{k-1}, q_i] \{ \pi[y(k) / Y_1^{k-1}] \}^{-1}, \quad (17)$$

where  $\pi[q_i / Y_1^{k-1}]$  – is the function known from the previous calculation cycle. The second factor in (16), under the condition of a fixed value  $q_i$ , can be represented as:

$$p[\varphi(k) = 1 / Y_1^k, q_i] = \frac{q_i \pi[y(k) / Y_1^{k-1}, \varphi(k) = 1, q_i]}{q_i \pi[y(k) / Y_1^{k-1}, \varphi(k) = 1, q_i] + (1 - q_i) \pi[y(k) / Y_1^{k-1}, \varphi(k) = N, q_i]}. \quad (18)$$

Since the result of observations  $y(k)$  doesn't explicitly depend on  $q_i$ , then  $\pi[y(k) / Y_1^{k-1}, \varphi(k) = 1, q_i] = \pi[y(k) / Y_1^{k-1}, \varphi(k) = 1]$ . The denominator (18) is the distribution density  $\pi[y(k) / Y_1^{k-1}, q_i]$ . Together, expressions (16) – (18) give the result:

$$p[\varphi(k) = 1 / Y_1^k] = \pi[y(k) / Y_1^{k-1}, \varphi(k) = 1] \{ \pi[y(k) / Y_1^{k-1}] \}^{-1} \int_0^1 q_i \pi[q_i / Y_1^k] dq_i, \quad (19)$$

and double averaging of the denominator (18) over  $q_i$  and  $\varphi(k)$  allows us to express it in terms of  $q_i$  and  $\pi[q_i / Y_1^k]$ ,  $\pi[y(k) / Y_1^{k-1}, \varphi(k) = i]$ , that is:

$$\begin{aligned} \pi[y(k) / Y_1^{k-1}] &= \int_0^1 \pi[q_i, y(k) / Y_1^{k-1}] dq_i = \int_0^1 \pi[q_i / Y_1^k] \pi[y(k) / Y_1^{k-1}, q_i] dq_i \\ &= \int_0^1 \{ q_i \pi[y(k) / Y_1^{k-1}, \varphi(k) = 1] + (1 - q_i) \pi[y(k) / Y_1^{k-1}, \varphi(k) = N] \} \pi[q_i / Y_1^{k-1}] dq_i \\ &= \sum_{i=1}^N \overline{q_i(k)} \pi[y(k) / Y_1^{k-1}, \varphi(k) = i], \quad i = 1, N; \text{ where } \overline{q_i(k)} = \int_0^1 q_i \pi[q_i / Y_1^k] dq_i; \quad \overline{q_N(k)} = 1 - \overline{q_1(k)}. \end{aligned}$$

Combining expressions (17) – (19), we obtain formula (15).

### 3.4. Synthesis methods for robust estimators in the presence of the observation channel abnormal bursts

Calculating pseudo Bayesian estimators as a linear combination of weighted particular type estimators:

$$s^*(k) = \sum_{i=1}^N s_i^*(k) p[\varphi(k) = i / Y_1^k] \quad (20)$$

is associated with the implementation of two parallel Kalman filters in operation. One of them is tuned to the hypothesis of the observation channel's normal state, and the other to its alternative - the presence of abnormal errors in the observation results. It is evident that the above form of obtaining the state vector's final estimate is accompanied by an increase in hardware and software costs. The fact that abnormal errors in the observation channel are modeled by a sudden increase in the parametric variable values  $\varphi(k)$ , much larger than unity, enables the design of estimators whose robust properties are implemented through structural and/or algorithmic shortcuts. Some of these will be the subject of further consideration, arranged in a hierarchical order.

**Robust estimator of structurally shortened type.** A structurally simplified, robust estimator will be synthesized by replacing the parallel operation of a pair of Kalman model-conditional filters with a single filter tuned to the hypothesis of the observation channel's normal state. To achieve this, it is proposed to introduce a block of correcting values for the matrix transfer coefficient into the feedback loop. The corrector's operation will depend on the switching algorithm combined with the circuit for calculating the posterior probability of the absence of anomalous errors. The formal-mathematical aspect of the synthesis issue is as follows. Let us decompose the algorithm for obtaining the final estimate of the system state vector (20) in the form:

$$s^*(k/k) = \left\{ \Sigma(k, k-1) s_1^*(k/k-1) + W_1(k) [y(k) - H(k) \Sigma(k, k-1) s_1^*(k/k-1)] \right\} p[\varphi(k) = 1/Y_1^k] + \left\{ \Sigma(k, k-1) s_N^*(k/k-1) + W_N(k) [y(k) - H(k) \Sigma(k, k-1) s_N^*(k/k-1)] \right\} p[\varphi(k) = N/Y_1^k] \quad (21)$$

Upon completion of the procedure for grouping similar terms (21) one can obtain the final estimate  $s^*(k/k)$ . The resulting form is identical to the estimate obtained by the Kalman filter method, where instead of the optimal transfer matrix  $W_i(k)$  its modified version  $W_M(k)$  is used.

$$s^*(k/k) = \Sigma(k, k-1) s^*(k/k-1) + W_M(k) [y(k) - H(k) \Sigma(k, k-1) s^*(k/k-1)], \quad (22)$$

where  $W_M(k) = \sum_{i=1}^N W_i(k) p[\varphi(k) = i/Y_1^k]$ .

Let us show that under the condition  $N \gg 1$ ,  $W_M(k)$  can be replaced by an approximate formula, the accuracy of which can be acceptable for the practical implementation.

$$W_M(k) \approx p[\varphi(k) = 1/Y_1^k] P_1(k/k) H(k) R_0^{-1}(k). \quad (23)$$

To do this, we write the transfer matrices  $W_1(k)$ ,  $W_N(k)$  as:

$$W_1(k) = P(k/k-1) H^T(k) [H(k) P(k/k-1) H^T(k) + R_0(k)]^{-1};$$

$$W_N(k) = P(k/k-1) H^T(k) [H(k) P(k/k-1) H^T(k) + N^2 R_0(k)]^{-1}.$$

Applying the matrix Woodbury identity  $CD(A \pm BCD)^{-1} = (C^{-1} \pm D^T A^{-1} B)^{-1} D^T A^{-1}$  one can obtain expressions that are convenient for performing the comparison procedure:

$$R_0^{-1}(k) [I - H(k) P(k/k-1) H^T(k)];$$

$$1/N^2 R_0^{-1}(k) [I - H(k) P(k/k-1) H^T(k)]. \quad (24)$$

Since the parametric variable  $\varphi_N(k)$  in the observation channel model in the presence of abnormal errors takes on a value much greater than unity, the component  $W_N(k)$  in expression (24) can be neglected, giving it a zero value. Therefore, the final assessment  $s^*(k/k)$  approximate equation that determines the estimator algorithm resistant to the abnormal errors influence is reduced to the form:

$$s^*(k/k) \approx \Sigma(k, k-1) s^*(k/k-1) + p[\varphi(k) = 1/Y_1^k] P(k/k) H(k) R_0^{-1}(k) [y(k) - H(k) \Sigma(k, k-1) s^*(k/k-1)]. \quad (25)$$

It should be noted that the introduced transmission matrix correction algorithm doesn't affect the operation of the filter in the absence of anomalous errors, since the probability is  $p[\varphi(k) = 1/Y_1^k] \equiv 1$  and its alternative is  $p[\varphi(k) = N/Y_1^k] \equiv 0$ . In this case, the synthesized structure degenerates into a standard Kalman filter by turning off the filtering channel for low-reliability observations. As a result, it remains possible to replace the classical filtering methods with more advanced methods capable of withstanding the influence of observation channel faults on the reliability of the state vector estimation results. In the case when the results of observations contain abnormal errors, the situation becomes diametrically opposite -  $p[\varphi(k) = 1/Y_1^k] \equiv 0$ ,  $p[\varphi(k) = N/Y_1^k] \equiv 1$ . Now, the part of the filter that is consistent to the absence abnormal errors hypothesis is turned off. The results of



filtering the alternative channel, despite the fact that  $p[\boldsymbol{\varphi}(k) = N / \mathbf{Y}_1^k] \equiv 1$ , are formed by a value close to zero  $\mathbf{W}_N(k)$  under the condition  $N \gg I$ . In fact, this means a break in the feedback loop and the transition of this filter section to the extrapolation mode, where the results of abnormal bursts observations are not used. Combining the detecting faults processes and evaluating their impact on the state vector final estimate  $s^*(\frac{k}{k})$  gives the synthesized device properties typical for parametric adaptation processes.

Let us analyze the structurally truncated estimates accuracy (25), based on the equation for the filtering errors covariance matrix (13). To do this, we write expressions for the model-conditional covariance matrices  $\mathbf{P}_i(\frac{k}{k})$

$$\mathbf{P}_1(\frac{k}{k}) = \mathbf{P}(\frac{k}{k-1}) - \mathbf{W}_1(k) \mathbf{H}(k) \mathbf{P}(\frac{k}{k-1}); \quad \mathbf{P}_N(\frac{k}{k}) = \mathbf{P}(\frac{k}{k-1}) - \mathbf{W}_N(k) \mathbf{H}(k) \mathbf{P}(\frac{k}{k-1}), \quad (26)$$

after that we will use them into (13) This makes it possible to write the weighted sum  $\sum_{i=1}^N \mathbf{P}_i(\frac{k}{k}) p[\boldsymbol{\varphi}(k) = i / \mathbf{Y}_1^k]$  in expanded form:

$$\mathbf{P}(\frac{k}{k-1}) p[\boldsymbol{\varphi}(k) = 1 / \mathbf{Y}_1^k] \mathbf{W}_1(k) \mathbf{H}(k) \mathbf{P}(\frac{k}{k-1}) - \{1 - p[\boldsymbol{\varphi}(k) = 1 / \mathbf{Y}_1^k]\} \mathbf{W}_N(k) \mathbf{H}(k) \mathbf{P}(\frac{k}{k-1}).$$

Taking into account (22), the second component of formula (13)  $[s^*(\frac{k}{k}) - s^*_1(\frac{k}{k})]$  can be written as:

$$\begin{aligned} & [s^*(\frac{k}{k}) - s^*_1(\frac{k}{k})] p[\boldsymbol{\varphi}(k) = N / \mathbf{Y}_1^k] = [\mathbf{W}_1(k) - \mathbf{W}_N(k)] \times \\ & \times [\mathbf{y}(k) - \mathbf{H}(k) \boldsymbol{\Sigma}(k, k-1) s^*(\frac{k-1}{k-1})] p[\boldsymbol{\varphi}(k) = N / \mathbf{Y}_1^k]. \end{aligned} \quad (27a)$$

In the same way, you can write the difference  $[s^*(\frac{k}{k}) - s^*_N(\frac{k}{k})]$

$$\begin{aligned} & [s^*(\frac{k}{k}) - s^*_N(\frac{k}{k})] p[\boldsymbol{\varphi}(k) = N / \mathbf{Y}_1^k] = [\mathbf{W}_1(k) - \mathbf{W}_N(k)] \times \\ & \times [\mathbf{y}(k) - \mathbf{H}(k) \boldsymbol{\Sigma}(k, k-1) s^*(\frac{k-1}{k-1})] p[\boldsymbol{\varphi}(k) = 1 / \mathbf{Y}_1^k]. \end{aligned} \quad (27b)$$

Taking into account expressions (27), we present the weighted sum (13) in expanded form, use the inequality  $\mathbf{W}_1(k) \gg \mathbf{W}_N(k)$  and reduce it to the following form:

$$\begin{aligned} & \sum_{i=1}^N \{ [s^*_i(\frac{k}{k}) - s^*(\frac{k}{k})] [s^*_i(\frac{k}{k}) - s^*(\frac{k}{k})]^T \} p[\boldsymbol{\varphi}(k) = i / \mathbf{Y}_1^k] = \\ & = p[\boldsymbol{\varphi}(k) = 1 / \mathbf{Y}_1^k] \{ 1 - p[\boldsymbol{\varphi}(k) = 1 / \mathbf{Y}_1^k] \}^2 \mathbf{W}_1(k) \mathbf{L}(k) \mathbf{W}_1^T(k) + \\ & + \{ 1 - p[\boldsymbol{\varphi}(k) = 1 / \mathbf{Y}_1^k] \} p^2[\boldsymbol{\varphi}(k) = 1 / \mathbf{Y}_1^k] \mathbf{W}_1(k) \mathbf{L}(k) \mathbf{W}_1^T(k) \end{aligned} \quad (28)$$

Next, we perform the procedure of grouping similar terms in (28) and combine them using (27). This will allow us to write the final result for the errors covariance matrix according to the structurally shortened algorithm

$$\begin{aligned} & \mathbf{P}(\frac{k}{k}) = \mathbf{P}(\frac{k}{k-1}) - \mathbf{W}_M(k) \mathbf{H}(k) \mathbf{P}(\frac{k}{k-1}) \\ & + \{ 1 - p[\boldsymbol{\varphi}(k) = 1 / \mathbf{Y}_1^k] \} \{ p[\boldsymbol{\varphi}(k) = 1 / \mathbf{Y}_1^k] \}^{-1} \mathbf{W}_M(k) \mathbf{L}(k) \mathbf{W}_M^T(k), \end{aligned} \quad (29)$$

where  $\mathbf{W}_M(k) = p[\boldsymbol{\varphi}(k) = 1 / \mathbf{Y}_1^k] \mathbf{P}_1(\frac{k}{k}) \mathbf{H}(k) \mathbf{R}_0^{-1}(k) -$  modified Kalman filter transfer matrix;  $\mathbf{L}(k) = [\mathbf{r}(k) \mathbf{r}^T(k)]$ , and  $\mathbf{r}(k) \triangleq [\mathbf{y}(k) - \mathbf{H}(k) \boldsymbol{\Sigma}(k, k-1) s^*(\frac{k-1}{k-1})]$  - residual signal introducing updated information into the synthesized filter structure. The synthesized filter transfer matrix is controlled by the a posteriori probability calculation unit using formula (18), where the value  $q_1(k)$  is priori known.

**Robust speed estimator.** It remains unchanged that the calculation of the a posteriori probability of the observation channel normal state  $p[\boldsymbol{\varphi}(k) = 1 / \mathbf{Y}_1^k]$  by formula (12) is still mathematically complex, and the distribution densities  $\pi[\mathbf{y}(k) / \mathbf{Y}_1^{k-1}, \boldsymbol{\varphi}(k) = i]$ ,  $i = 1, N$  can be multidimensional and not belong to the class of normal distributions. In this case the formation of a matrix gain control signal  $\mathbf{W}_M(k)$  will be too late, and doesn't contribute to the estimation goal achievement for highly dynamic processes and a high frequency of observations results updating. The author proposes to replace the calculate values procedure  $p[\boldsymbol{\varphi}(k) = 1 / \mathbf{Y}_1^k]$  by a binary selector circuit in order to overcome the above-mentioned computational difficulties. In this regard, we make the assumption that the distribution densities  $\pi[\mathbf{y}(k) / \mathbf{Y}_1^{k-1}, \boldsymbol{\varphi}(k) = i]$ ,  $i = 1, N$  belong to the class of normal distributions and have the following parameters:

$$\begin{aligned} & \pi[\mathbf{y}(k) / \mathbf{Y}_1^{k-1}, \boldsymbol{\varphi}(k) = 1] = N [\mathbf{H}(k) s^*(\frac{k-1}{k-1}), \mathbf{H}(k) \mathbf{P}(\frac{k-1}{k-1}) \mathbf{H}^T(k) + \mathbf{R}_0(k)]; \\ & \pi[\mathbf{y}(k) / \mathbf{Y}_1^{k-1}, \boldsymbol{\varphi}(k) = N] = N [\mathbf{H}(k) s^*(\frac{k-1}{k-1}), \mathbf{H}(k) \mathbf{P}(\frac{k-1}{k-1}) \mathbf{H}^T(k) + N^2 \mathbf{R}_0(k)]. \end{aligned} \quad (30)$$

Without losing generality of the results obtained, we restrict ourselves to the case of single-input single-output discrete systems, where the observation matrix will have the form  $\mathbf{H}(k) = [1, 0, \dots, 0]$ . This will give a simplified expression for the posterior probability  $p[\boldsymbol{\varphi}(k) = 1/Y_1^k]$ :

$$p[\boldsymbol{\varphi}(k) = 1/Y_1^k] = q_1(k) [\boldsymbol{\Xi}_1(\frac{k}{k-1})]^{-0.5} \exp\left\{-\frac{r^2(k)}{2[\boldsymbol{\Xi}_1(\frac{k}{k-1})]}\right\} \times \left\{ q_1(k) [\boldsymbol{\Xi}_1(\frac{k}{k-1})]^{-0.5} \exp\left\{-\frac{r^2(k)}{2[\boldsymbol{\Xi}_1(\frac{k}{k-1})]}\right\} + [1 - q_1(k)] [\boldsymbol{\Xi}_N(\frac{k}{k-1})]^{-0.5} \exp\left\{-\frac{r^2(k)}{2[\boldsymbol{\Xi}_N(\frac{k}{k-1})]}\right\} \right\}^{-1}. \quad (31)$$

where  $r(k) \triangleq \left[ y(k) - y^* \left( \frac{k}{k-1} \right) \right]$  – difference signal  $\boldsymbol{\Xi}_i(\frac{k}{k-1}) = P_{11}(k/k-1) + i^2 R_0(k)$ ,  $i=1, N$  – correlation matrix of the difference signal, consistent with the accepted hypotheses  $H_1$  and its alternatives  $H_N$  for  $N \gg 1$ ;  $P_{11}(k/k-1)$  – extrapolation error variance one step ahead.

Presently let's make an assumption that if the implementation of the observations sequence of observations  $Y_1^k$  is available, the value  $p[\boldsymbol{\varphi}(k) = 1/Y_1^k]$  at each step of the computational process  $k$  can take only two values: one - the current values of  $y(k)$  fall into the value range  $\Delta y(k)$  formed by the inequality  $|r(k)| \leq \Delta y(k)$  and zero otherwise. The size of the range is determined by the value area where the probability distribution density  $\pi[y(k)/Y_1^{k-1}, \boldsymbol{\varphi}(k) = 1]$  is non-zero. Further considerations are based on the observation channel model (3),

where the anomalous error mode is described by the intuitive relation  $\Xi_N \left( \frac{k}{k-1} \right) \gg \Xi_1 \left( \frac{k}{k-1} \right)$ . Due to this factor, the density  $\pi[y(k)/Y_1^{k-1}, \boldsymbol{\varphi}(k) = N]$  remains constant value in the range  $\pm \Delta y(k)$ , which can be considered as

$$\pi[y(k)/Y_1^{k-1}, \boldsymbol{\varphi}(k) = N] = \left\{ 2\pi \left[ P_{11}(\frac{k}{k-1}) + N^2 R_0(k) \right] \right\}^{-0.5}, \quad (32)$$

and the probability of an incorrect solution can be calculated approximately  $p[y(k) \in 2\Delta y(k)] \approx \Delta y(k) \sqrt{\frac{2}{\pi [P_{11}(\frac{k}{k-1}) + N^2 R_0(k)]}}$ .

An analytical expression for the confidence interval  $\pm \Delta y(k)$  is found by introducing a small positive number  $\varepsilon > 0$ , which describes the difference between unity and the posterior probability current value  $p[\boldsymbol{\varphi}(k) = 1/Y_1^k]$  in equation (31). If we use formula (32), then the normalized solution of the above equation will have the form:

$$\frac{\Delta y(k)}{\boldsymbol{\Xi}_1(\frac{k}{k-1})} = \left\{ 2 \ln \left[ \frac{\boldsymbol{\Xi}_N(\frac{k}{k-1})}{\boldsymbol{\Xi}_1(\frac{k}{k-1})} \right] \frac{\varepsilon}{(1-\varepsilon)} \frac{q_1(k)}{[1 - q_1(k)]} \right\}^{0.5}. \quad (33)$$

Considering formula (32), it is easy to see that the width of the confidence interval  $\Delta y(k)$  is a variable, since the extrapolated estimates  $y^*(\frac{k}{k-1})$  are constantly refined due to the receipt of new observational results. In this regard, on the way to finding optimal values  $\Delta y(k)$ , there are difficulties of mathematical calculation. In this work, this problem was solved by performing a computational experiment using the Monte Carlo method, where the value of the confidence interval  $\Delta y(k)$  was chosen from the series  $\boldsymbol{\Xi}_1(\frac{k}{k-1})$ ,  $2\boldsymbol{\Xi}_1(\frac{k}{k-1})$ ,  $3\boldsymbol{\Xi}_1(\frac{k}{k-1})$ . The most reliable results were obtained for the option  $\Delta y(k) = 2\boldsymbol{\Xi}_1(\frac{k}{k-1})$ , the accuracy of the obtained estimates was calculated as:

$$\mathbf{P}(\frac{k}{k}) = \begin{cases} \mathbf{P}(\frac{k}{k-1}) [\mathbf{I} - \mathbf{W}_1(k) \mathbf{H}(k)], & y(k) \in 2\Delta y; \\ \mathbf{P}(\frac{k}{k-1}), & y(k) \notin 2\Delta y. \end{cases} \quad (34)$$

In conclusion, it is fair to state that the employment of binary logic rules in the selector circuit, instead of a posterior probability calculation unit  $p[\boldsymbol{\varphi}(k) = 1/Y_1^k]$ , significantly improves the performance of the estimator. This is achieved by reducing the amount of required RAM and the execution time for specific operations. For instance, if a decision is made at this stage that no abnormal errors exist (thus making the value of the posterior probability calculation unit  $\boldsymbol{\varphi}(k)$  equal to one), the filtering process uses the Kalman filter, which is tuned to the nominal operating mode of the observation channel. In the alternative case, where abnormal errors are detected, the feedback loop is opened, and the filter switches to extrapolation mode, avoiding the use of unreliable data. It's

important to note that these advantages come at the expense of some loss in accuracy. However, this trade-off is often acceptable in practice due to the considerable benefits in efficiency and computational resources. The proposed selector algorithm can be interpreted as a statistical detector of abnormal bursts in individual observation results. The quality metrics for this algorithm are determined by the probabilities of making erroneous decisions of the first and second kinds.

**Synthesis of a linear type robust estimator** was carried out with the aim of developing an extremely simplified method for obtaining state vector estimates with limited fault influence tolerance, however is algorithmically simple and fast. The main stages of synthesis were reduced to the following steps:

1. To remain under the terms of the Bayesian approach, the state vector optimal estimate in the form of a posteriori mean was used. The optimality of the estimate consisted of minimizing the estimation errors variance using a quadratic cost function. Additionally, it was assumed that mathematical models were available to describe the system dynamics and the procedure for generating output data with observation channel abnormal errors (4)-(5).

2. The posterior distribution density in  $\pi[s(k)/Y_1^k]$  implicitly depends on the parametric variable and is generally not Gaussian, but refers to distributions of the poly-Gaussian type. Using the Bayes formula allows you to present it in expanded form:

$$\pi[s(k)/Y_1^k] = \sum_{i=1}^N \frac{\pi[s(k)/Y_1^{k-1}] \pi[y(k)/Y_1^{k-1}, s(k), \varphi(k)=i]}{\pi[y(k)/Y_1^{k-1}, \varphi(k)=i]} \times \frac{q_i(k) \pi[y(k)/Y_1^{k-1}, \varphi(k)=i]}{\pi[y(k)/Y_1^{k-1}]} \quad (35)$$

Distribution density  $\pi[s(k)/Y_1^{k-1}]$  according to (5) from current  $\varphi(k)$  doesn't depend, but  $\pi[y(k)/Y_1^{k-1}]$  can be computed using the properties of the conditional mean value

$$\pi[y(k)/Y_1^{k-1}] = E_{\varphi(k)} \{ \pi[y(k)/Y_1^{k-1}, \varphi(k)=i] \} = \sum_{i=1}^N p[\varphi(k)=i/Y_1^{k-1}] \pi[y(k)/Y_1^{k-1}, \varphi(k)=i] \quad (36)$$

and also loses dependence on  $\varphi(k)$ ,  $p[\varphi(k)=i/Y_1^{k-1}]$  is an a priori given value since the sequence elements  $\{\varphi(1), \varphi(2), \dots, \varphi(k)\}$  behind the assumption are statistically independent values. This makes it possible to write the posterior distribution density (35) in the form:

$$\pi[s(k)/Y_1^k] = \frac{\pi[s(k)/Y_1^{k-1}]}{\pi[y(k)/Y_1^{k-1}]} \sum_{i=1}^N q_i(k) \pi[y(k)/Y_1^{k-1}, s(k), \varphi(k)=i] \quad (37)$$

3. A necessary condition for the current estimate  $s^*(k)$  to belong to the class of linear estimates is a linear-functional dependence on the observation results and the filtering errors covariance matrix  $P(k)$  should be calculated only on the priori data basis.

To do this, we exclude the blocks for calculating posterior probabilities  $p[\varphi(k)=i/Y_1^{k-1}]$  from expression (36) and replace them by a priori known values  $p[\varphi(k)=i] = q_i(k)$ ,  $i=1, N$ . Then expression (37) takes the form:

$$\pi[s(k)/Y_1^k] = \pi[s(k)/Y_1^{k-1}] \left( \frac{\sum_{i=1}^N q_i(k) \pi[y(k)/Y_1^{k-1}, s(k), \varphi(k)=i]}{\sum_{i=1}^N q_i(k) \pi[y(k)/Y_1^{k-1}, \varphi(k)=i]} \right) \quad (38)$$

4. The next step is to approximate the distribution densities included in the numerator and denominator of expression (38) by Gaussian distributions with equivalently recalculated parameters. The distribution density  $\pi[s(k)/Y_1^{k-1}]$  is determined by the values obtained from the previous calculation cycle and the system dynamics model (5). Therefore, the parameters  $s^*(k-1)$  and  $P(k-1)$  can be considered known and independent of the parametric variable values  $\varphi(k)$ . Considering these remarks and referring to formulas (10), we write the final expression for the posterior distribution density  $\pi[s(k)/Y_1^k]$ :

$$\pi[s(k)/Y_1^k] = \frac{N[s^*(k-1), P(k-1)] \times N\{H(k)s(k), [q_i(k)(1-i^2) + i^2]R(k)\}}{N\{H(k)s^*(k-1), H(k)P(k-1)H^T(k) + [q_i(k)(1-i^2) + i^2]R(k)\}} \quad (39)$$

5. Now, if we introduce the notation for the modified noise covariance matrix  $\mathbb{R} \triangleq \left[ q_i(k)(1-i^2) + i^2 \right] \mathbf{R}_0(k)$ , then the synthesized filter becomes structurally identical to the Kalman filter. However, it remains only suboptimal, since the ratio  $\mathbb{R} \geq \mathbf{R}_0(k)$  is always preserved. Namely, in this context the filtering accuracy should be estimated by the expression valid for an arbitrary linear filter with a non-optimal transfer matrix:

$$\begin{aligned}
 \mathbf{s}^* \left( \frac{k}{k-1} \right) &= \Sigma(k, k-1) \mathbf{s}^* \left( \frac{k-1}{k-1} \right); \\
 \mathbf{P} \left( \frac{k}{k-1} \right) &= \Sigma(k, k-1) \mathbf{P} \left( \frac{k-1}{k-1} \right) \Sigma^T(k, k-1) + \mathbf{Q}(k-1); \\
 \mathbf{W}_L(k) &= \mathbf{P} \left( \frac{k}{k-1} \right) \mathbf{H}^T(k) \left\{ \mathbf{H}(k) \mathbf{P} \left( \frac{k}{k-1} \right) \mathbf{H}^T(k) + \left[ q_i(k)(1-i^2) + i^2 \right] \mathbf{R}_0(k) \right\}^{-1}; \\
 \mathbf{s}^* \left( \frac{k}{k} \right) &= \mathbf{s}^* \left( \frac{k}{k-1} \right) + \mathbf{W}_L(k) \left[ \mathbf{y}(k) - \mathbf{H}(k) \mathbf{s}^* \left( \frac{k}{k-1} \right) \right]; \\
 \mathbf{P} \left( \frac{k}{k} \right) &= \left[ \mathbf{I} - \mathbf{W}_L(k) \mathbf{H}(k) \right] \mathbf{P} \left( \frac{k}{k-1} \right) \left[ \mathbf{I} - \mathbf{W}_L(k) \mathbf{H}(k) \right]^T + \\
 &+ \mathbf{W}_L(k) \left\{ \left[ q_1(1-N^2) + N^2 \right] \mathbf{R}_0(k) \right\} \mathbf{W}_L^T(k).
 \end{aligned} \tag{40}$$

In practice, prior and posterior data often have significant differences. As a result, the synthesized filter provides the minimum possible protection against the influence of abnormal bursts in the observation results by simply narrowing the bandwidth. Consequently, there is an increase in the level of dynamic errors during the filtration process. It should be emphasized that formulas (40) were obtained based on the use of the full matrix square complement procedure and the smoothing properties of the conditional expectation.

#### 4. Simulation results

Statistical Monte Carlo modeling was conducted to verify the performance of the proposed estimation algorithms and their comparative analysis. As an illustrative example, a model of an aircraft's movement during an approach in the planning phase was used. The landing trajectory was formed using microwave landing system (MLS) electronic equipment. In this case, the task of maneuvering is to keep the aircraft on the selected landing trajectory, approximately at a  $-3^\circ$  angle to the runway plane, using a glide path radio beacon. The second-order Singer model [29] was chosen as the nominal mathematical model of the aircraft elevation angle changes and the corresponding transition matrix in expression (5) has the form  $\Sigma(k+1, k) = \begin{bmatrix} 1 & T \\ 0 & 1 \end{bmatrix}$ , where  $T$ —sampling interval equal to 0.0247s corresponding to the glide path beacon scanning frequency of 40.5 Hz. Other a priori data are given in Table. 1. A detailed substantiation of the data can be found in the [30].

**Table 1.** A priori data for the planning phase

$  \mathbf{s}(0) = \begin{bmatrix} 3.200 \\ 0.010 \end{bmatrix}; \quad \mathbf{s}^* (\%) = \begin{bmatrix} 2.800 \\ 0.008 \end{bmatrix}; \quad \mathbf{P} (\%) = \begin{bmatrix} 0.700 & 0.000 \\ 0.000 & 0.040 \end{bmatrix}; \quad \mathbf{R}(k) = 0.0064;  $
$  \mathbf{Q}(k) = 0.0009; \quad \mathbf{H} = [1 \ 0]; \quad T = 0.0247; \quad N_p = 50; \quad q_1(k) = 0.85; \quad N = 1, 20.  $

The effective precision evaluation of the proposed estimation algorithms was performed by comparing the accuracy of corresponding statistical characteristics with the statistical characteristics of the reference standard Kalman filter. The characteristics were calculated through repeated simulation of the algorithm under study as part of the computational process. Subsequently, probabilistic averaging over the set was replaced by calculating arithmetic mean values  $s$  using the following formulas:

$$\begin{aligned}
 E \{ \Delta \mathbf{s}(k) \} &= \frac{1}{N_p} \sum_{i=1}^{N_p} \left[ s_i(k) - s_i^* \left( \frac{k}{k} \right) \right] = \overline{\Delta \mathbf{s}(k)}; \\
 E \{ \Delta \mathbf{s}(k) \Delta \mathbf{s}(k)^T \} &= \frac{1}{N_p - 1} \sum_{i=1}^{N_p} \left[ s_i(k) - s_i^* \left( \frac{k}{k} \right) \right]^2 = \overline{\Delta \mathbf{s}(k)^2}; \\
 E \left\{ \left[ \Delta \mathbf{s}(k) - \overline{\Delta \mathbf{s}(k)} \right] \left[ \Delta \mathbf{s}(k) - \overline{\Delta \mathbf{s}(k)} \right]^T \right\} &= \overline{\Delta \mathbf{s}(k)^2} - \left[ \overline{\Delta \mathbf{s}(k)} \right]^2,
 \end{aligned}$$

where  $N_p$  – implementations number.

A comparative analysis of the evaluation results was carried out under the most identical conditions - the same implementations of random processes  $\mathbf{y}(k), \mathbf{s}(k), \varphi(k), \mathbf{w}(k), \mathbf{v}(k)$  were fed to the inputs of all the devices under study. The accuracy of the simulation results was evaluated by two parameters: the reliability of the obtained estimates  $\eta$  and the width of the confidence interval  $\Delta$ . In the course of statistical experiments, it is common practice to set the estimation reliability from the standard series 0.9, 0.95, 0.99, 0.999, and the value of  $\Delta$  is calculated using the formula:

$$[\mathbf{P}^*(k/k)]^{0.5} (1 - \Delta) < [\mathbf{P}(k/k)]^{0.5} < [\mathbf{P}^*(k/k)]^{0.5} (1 + \Delta)$$

where  $[\mathbf{P}^*(k/k)]^{0.5}, [\mathbf{P}(k/k)]^{0.5}$  – sample and general RMS, respectively;  $\Delta$  - the width of the confidence interval, depends on the number of realizations and the reliability  $\eta$ . According to the a priori given values  $\eta$  and  $\Delta$ , one can find the value  $N_p$  that guarantees the given reliability. For example, at  $\eta = 0.95$  and  $\Delta = 20\%$ , the required number of realizations  $N_p$  is at least 50. For further modeling, let's take  $N_p=50$ . Fig. 2a shows the aircraft elevation angle estimates obtained using the standard Kalman filter (KF) and the process of creating pseudo Bayesian estimates (PBF) in the presence of abnormal bursts in the observation results (OR).

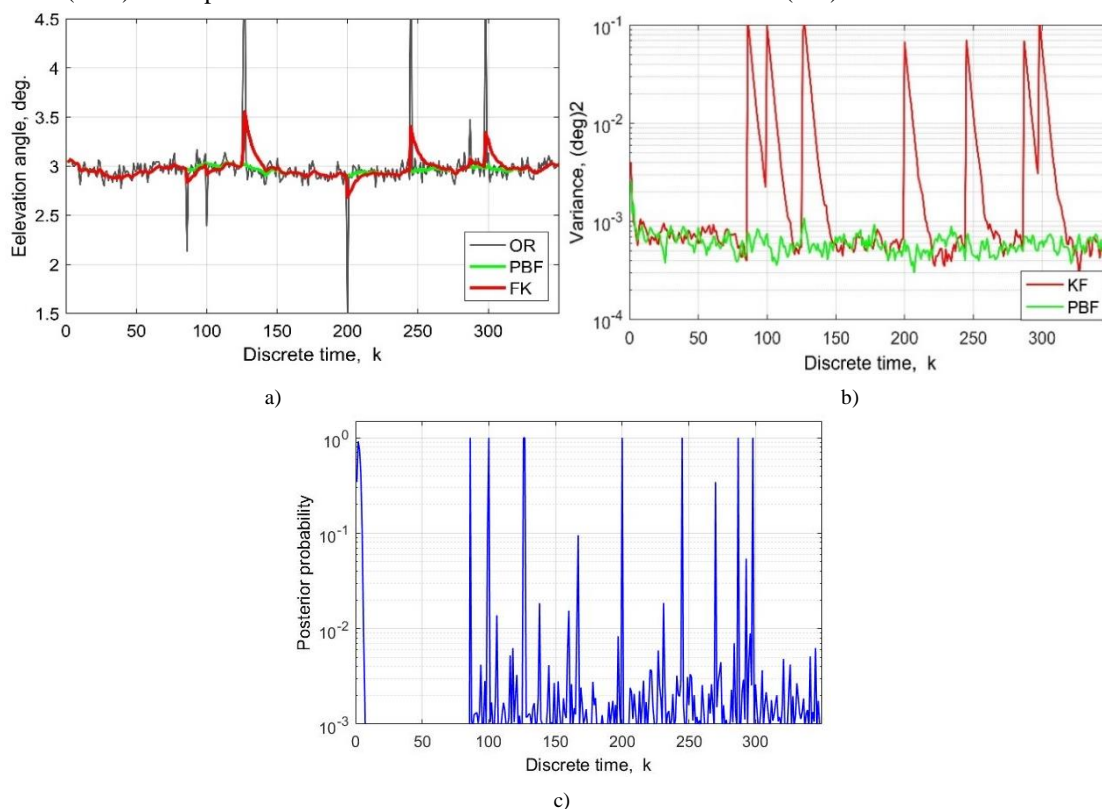


**Figure 2.** The aircraft elevation angle estimation results: a) the aircraft elevation angle dynamics; b) the filter error variance; c) the posteriori probability dynamics

It is easy to see that, under these conditions, it is not advisable to use the standard Kalman filter due to its inability to adapt to the influence of abnormal bursts in the observation results, in contrast to pseudo-Bayesian-type estimates. This is confirmed by Fig. 2b, which shows the dependences of the error's variance in the aircraft elevation angle estimation. At some points in time, the difference in accuracy can be more than ten times larger. The results of detecting abnormal bursts in the observation sequence for a separately accepted implementation are shown in Fig. 2c in the form of posteriori probability  $p[\varphi(k) = N / \mathbf{Y}_1^k]$  under the initial conditions indicated in Table 1.

Modeling of the adaptive estimation algorithm was conducted under the condition that the posterior distribution  $\pi[q_1 / \mathbf{Y}_1^k]$  was approximated on the interval  $[0, 1]$  by a uniform grid consisting of 50 points. The average value of the observation channel normal state probability was calculated based on the ratio  $\overline{q_1(k)} = 0.02 \sum_{i=0}^{49} q_i \pi[q_i / \mathbf{Y}_1^k]$ . In Figure 3a, some of the possible implementations of the aircraft elevation angle primary observations, containing abnormal bursts, and the result of its processing by the adaptive estimation algorithm are shown. Figure 3b displays the graph of its accuracy.

Theoretical values  $P_{11}(k/k)$  were calculated using formulas (11), (13), and the actual values  $P_{11}(k/k)$  were obtained by averaging realizations of adaptive filter estimates. The initial discrepancy between the theoretical and experimental values in the computational process's first cycles is explained by the effect of the adaptive filter's self-learning in order to overcome the initial a priori uncertainty. This is confirmed by Figure 3c, where the a posteriori probability (PP) of the occurrence of anomalous errors is presented, and its average value is time-varying (AvPP). From the above results, we can conclude that after studying the anomalies' statistics, the convergence process to the true value of the normal state observation channel probability (0.85) occurs very slowly. This is confirmed by the time variation process of the distribution density  $\pi[q1/Y1k]$ , shown in Figure 4.

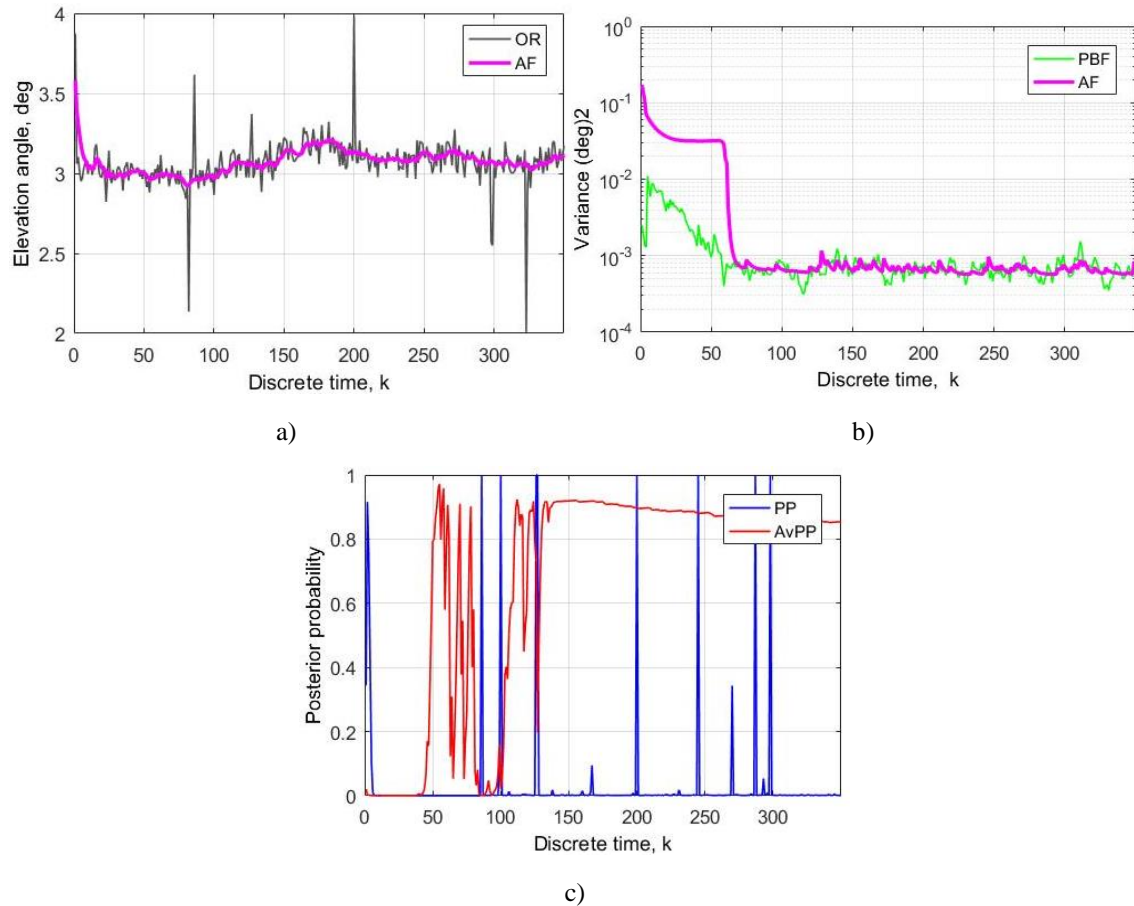


**Figure 3** AF evaluation result a); AF error variance b); the posteriori probability dynamics and average value c).

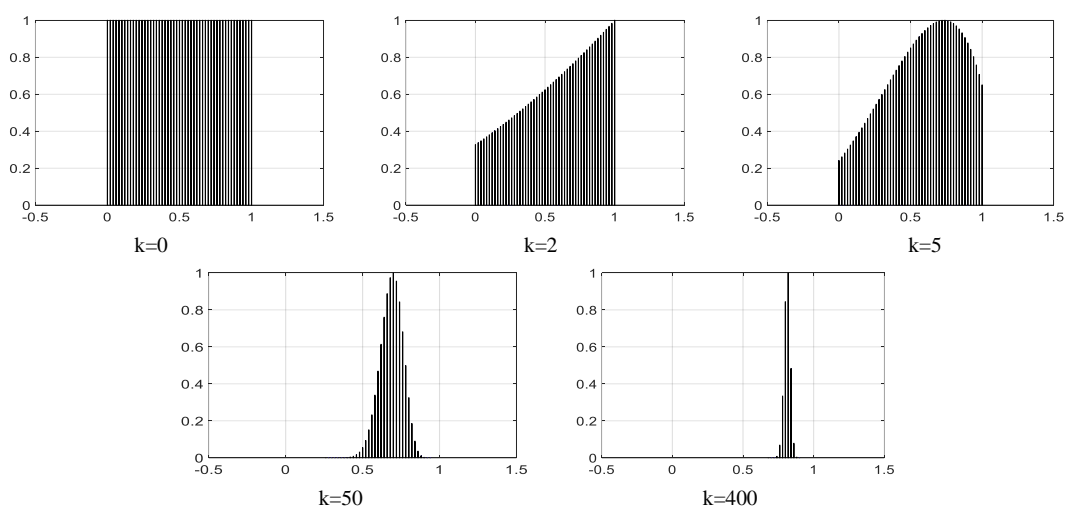


**Figure 4.** The probability distribution density evolution  $\pi[q1/Y1k]$  of the observation channel normal state during of the adaptation process.

Therefore, it is advisable to use adaptive estimation algorithms in cases where the issue of optimizing the transient process is not so significant, and the dynamics of information parameters change over time more slowly compared to the adaptive filter dynamics. The simulation results for a group of robust devices are shown in Fig. 5-6.

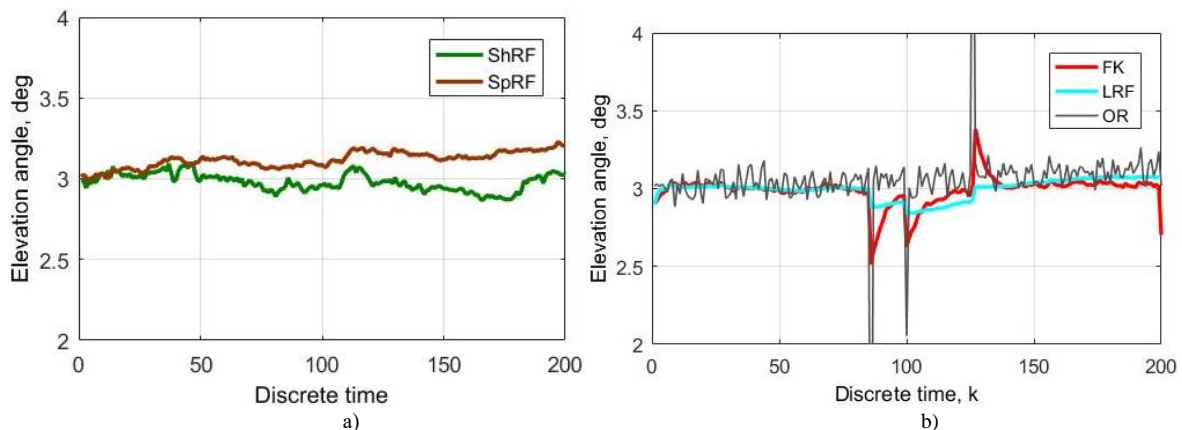


**Figure 5.** Results of aircraft elevation angle estimation by robust filters: a) the linear robust filter (LRF); b) the structurally shortened type robust filter (ShRF) and the increased speed Robust filterkhol(SpRF).

Figure 5a illustrates the results of the aircraft elevation angle estimation by a Linear Robust Filter (LRF). The LRF's resistance to anomalous errors is provided by adjusting the transmission matrix of the Kalman filter based on available a priori data. When the statistics of anomalies do not align with the a priori data, this filter behaves very similarly to the FK (Fault Kalman) filter. However, as the observation results  $Y1k$  accumulate and the statistics of abnormal bursts begin to align with the a priori data, formula (40a) takes these into account when calculating the transfer matrix  $W_L(k)$ . As a result, the forced narrowing of the filter's bandwidth provides the minimum possible level of stability of the linear filter against abnormal bursts in the observation results. However, this adjustment also leads to an excessively passive filter. Therefore, in the absence of anomalies, there is a nearly two-fold drop in estimation accuracy, observed both in the transient and steady states, when compared to the standard Kalman filter (as depicted in Figures 6a and 6b). However, in the presence of abnormal bursts, the gain in accuracy relative to the standard filter is within 2-2.5 times. It should be noted, however, that when compared to the pseudo-Bayesian estimate, the accuracy of the LRF decreases by approximately 8-10 times.

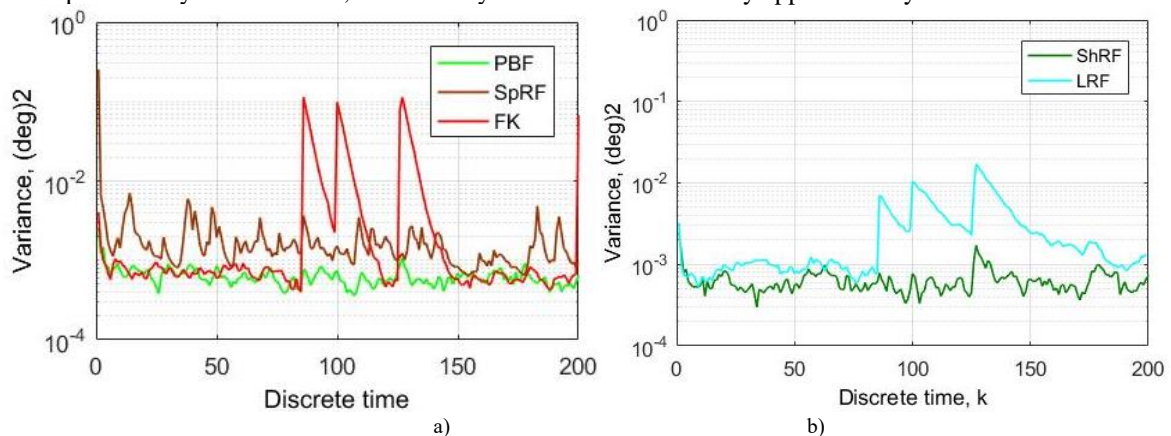


**Figure 6.** The estimation accuracy of the aircraft elevation angle by increased resilience filters: a) SpRF; b) ShRF, LRF.

Figure 5b displays the aircraft's elevation angle estimation results obtained through the use of a Structurally Shortened Type Robust Filter (SSTRF) and an Increased Speed Robust Filter (ISRF). The slight discrepancy observed between these curves can be attributed to the distinct methods employed to achieve robustness against abnormal errors. In the case of the SSTRF, robustness is provided through the use of an extrapolation mode. For the ISRF, robustness is assured via a rejection procedure, the quality of which depends on the selected duration of the control signal. When comparing their performance metrics to the quality of Bayesian estimates (shown in Fig. 6a), it can be noted that the ISRF (Fig. 6a) is less preferred due to a three to five-fold loss in accuracy. On the other hand, the SSTRF's loss in accuracy (Fig. 6b) stands at approximately 40-50% when compared to the accuracy of the pseudo Bayesian estimates.

The considered algorithms efficiency concerning the measurement channel anomalies was estimated by means of the introduced coefficient  $K_{ef}$

$$K_{ef}(k) = \sigma_{st}^2(k) / \sigma_i^2(k)$$

where,  $\sigma_{st}^2(k)$  – is the variance of the Kalman filter as a standard;  $\sigma_i^2(k)$  – is the considered filter variance. The comparison results are shown in Fig. 7.

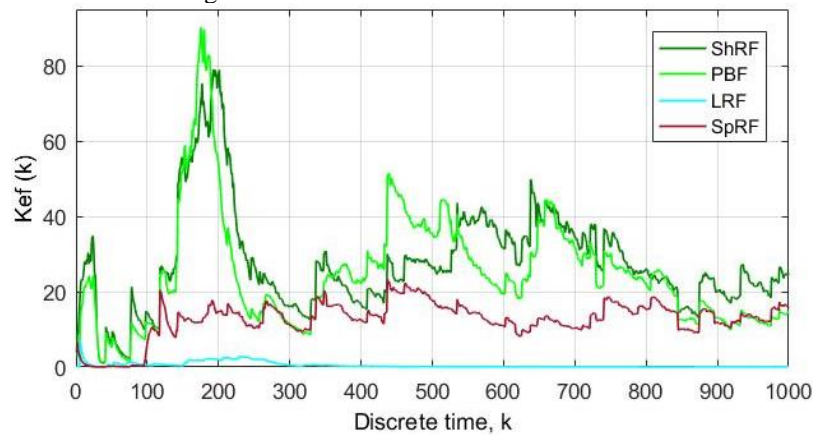


Figure 7. The error protection efficiency achieved by the proposed filters

The computational costs associated with the practical implementation of the proposed filtering methods can be determined by the number of mathematical operations performed, namely multiplication and addition. The number of such operations was computed using the well-known method described in [31]. The results of these calculations are presented in summary table 2.

Table 2. The computational costs estimates per one iterative cycle of the filtration process

Considered filters	Multiplications	Additions	Memory cells	Multiplications (norm. to FK)	Additions (norm. to FK)	Accuracy gain (TM)	Accuracy gain (SM)
KF	47	32	16	1	1	1	1
PBF	84	41	27	1,79	1,28	20–85	30–40
AF	584	292	133	12,43	9,13	30–60	≈30
ShRF	49	37	23	1,06	1,16	20–80	20–30
SpRF	53	36	19	1,13	1,17	15–20	12–15
LRF	47	38	16	1	1	0,8–2,5	0,3–0,5

## 5. Conclusions

In this paper, we develop a novel approach to filter design, aiming to generate control object state estimates capable of withstanding fault actions in the measurement sub-system. Considering the above, we can make the following observations: The most effective strategy for designing a filter that can handle unusual errors in an observation channel involves the use of pseudo-Bayesian estimates. The gain in estimation accuracy, in comparison to the Kalman filter in transient mode, is approximately 60–80 times, and reaches up to 30–40 times in the steady state. However, the computational costs for the multiplication and addition operations are 1.8 times and 1.3 times higher, respectively, compared to the standard Kalman Filter (KF). Hence, the application of the standard Kalman filter under these conditions seems impractical. In the practical example considered, our synthesized adaptive filter produces estimates of the aircraft's elevation angle during the self-learning stage. Although these estimates are almost twice as inaccurate as the pseudo-Bayesian ones, their accuracy rates become almost equal by the end of the learning process. Overcoming a priori uncertainty requires an order of magnitude more computational costs, and we observed a very slow convergence of the fault probability estimates in the measurement channel. In many practical real-time applications (for instance, tracking an aircraft's movement during an approach), there often exists a need to strike a balance between accuracy and system response speed due to hardware limitations. We have successfully developed simplified robust algorithms to address this issue.



When assessing the aircraft's elevation angle, the superiority of the ShRF filter accuracy over the KF reaches 50–70 times in transient mode and decreases to 20–25 times in the steady state. The ShRF incurs an accuracy loss of 30–40% relative to the PBF, while the increase in computational costs compared to the KF does not exceed 10–15%. Under the same conditions, the SpR filter provides a gain in accuracy compared to the KF up to 12–15 times, regardless of the filter operation mode. Its primary advantage is the absence of delay in data formation, while the computational overhead is comparable to ShRF. The last of the synthesized filters, LRF, is capable of withstanding the influence of anomalous errors only in the portion of the filtration process that is consistent with the available a priori data. The gain in accuracy compared to the standard is within 2–2.5 times. In the absence of measurement errors, this filter's estimation quality is inferior to the KF due to the suboptimal choice of the matrix transfer coefficient, leading to the appearance of dynamic errors. Despite requiring similar computational resources as the LRF, it does not demand any substantial reconstruction, except for correcting the measurement noise covariance matrix according to the available a priori data.

## Acknowledgments

The authors express their appreciation to the colleagues from Vinnytsia National Technical University, Lviv Polytechnic National University and Silesian University of Technology for helping with this work, and acknowledges the valuable suggestions from the peer reviewers.

## Conflict of interest

There is no conflict of interest for this study.

## References

- [1]. Varga. Solving Fault Diagnosis Problems: Linear Synthesis Techniques. Studies in Systems, Decision and Control. Vol. 84. Springer International Publishing; 2017. p. 394.
- [2]. Blanke M, Kinnaert M, Lunze J, Staroswiecki M. Diagnosis and Fault Tolerant Control. Springer-Verlag; 2016. p. 695.
- [3]. Thirumarimurugan M, Bagyalakshmi N, Paarkavi P. Comparison of fault detection and isolation methods: A review. 10th International Conference on Intelligent Systems and Control (ISCO); 2016. p. 1–6.
- [4]. Tipaldi M, Bruenjes B. Survey on Fault Detection, Isolation, and Recovery Strategies in the Space Domain. *J Aerospace Inf Syst.* 2015;12(2):235–56.
- [5]. Frank PM. Fault diagnosis in dynamic systems using analytical and knowledge-based redundancy - a survey and some new results. *Automatica.* 1990;26(3):459–74.
- [6]. Volovik Y, Krylik LV, Kobylanska IM, Kotyra A, Amirgaliyeva S. Methods of stochastic diagnostic type observers. *Proc SPIE Photonics Applications in Astronomy, Communications, Industry, and High-Energy Physics Experiments.* 2018 Oct;10808:108082X.
- [7]. Patton RJ, Uppal FJ, Lopez-toribio C. Soft Computing Approaches to Fault Diagnosis for Dynamic Systems: A Survey. *IFAC Proc Vol.* 2000;33(11):303–15. doi: 10.1016/S1474-6670(17)37377-9.
- [8]. Escobet T, Bregon AB, Puig P. Fault Diagnosis of Dynamic Systems: Quantitative and Qualitative Approaches. Springer International Publishing; 2019. p. 462.
- [9]. Baranowski J, Bania P, Prasad I, Cong T. Bayesian fault detection and isolation using Field Kalman Filter. *EURASIP J Adv Signal Process.* 2017.
- [10]. Gao G, Zhong Y, Gao S, Gao B. Double-Channel Sequential Probability Ratio Test for Failure Detection in Multisensor Integrated Systems. *IEEE Trans Instrumentation Measurement.* 2021;70:1–14. Art no. 3514814. doi: 10.1109/TIM.2021.3072674.
- [11]. Gao G, Gao B, Gao S, Hu G, Zhong Y. A Hypothesis Test-Constrained Robust Kalman Filter for INS/GNSS Integration With Abnormal Measurement. *IEEE Trans Vehicular Technology.* 2023 Feb;72(2):1662–73. doi: 10.1109/TVT.2022.3209091.
- [12]. Gao B, Hu G, Zhu X, Zhong Y. A Robust Cubature Kalman Filter with Abnormal Observations Identification Using the Mahalanobis Distance Criterion for Vehicular INS/GNSS Integration. *Sensors (Basel).* 2019 Nov;19(23):5149. doi: 10.3390/s19235149.

- [13]. Gao B, Hu G, Zhong Y, Zhu X. Cubature Kalman Filter With Both Adaptability and Robustness for Tightly-Coupled GNSS/INS Integration. *IEEE Sensors J.* 2021 Jul;21(13):14997-15011. doi: 10.1109/JSEN.2021.3073963.
- [14]. Hu G, Gao B, Zhong Y, Ni L, Gu C. Robust Unscented Kalman Filtering With Measurement Error Detection for Tightly Coupled INS/GNSS Integration in Hypersonic Vehicle Navigation. *IEEE Access.* 2019;7:151409-21. doi: 10.1109/ACCESS.2019.2948317.
- [15]. Zhu X, Gao B, Zhong Y, Gu C, Choi KS. Extended Kalman filter for online soft tissue characterization based on Hunt-Crossley contact model. *J Mech Behav Biomed Mater.* 2021 Nov;123:104667. doi: 10.1016/j.jmbbm.2021.104667. Epub 2021 Jul 1.
- [16]. Zolghadri, Henry D, Cieslak J, Efimov D, Goupil P. *Fault Diagnosis and Fault-Tolerant Control and Guidance for Aerospace Vehicles: From Theory to Application.* Springer-Verlag; 2014.
- [17]. Ossmann D, Varga A. Detection and identification of loss of efficiency faults of flight actuators. *Int J Appl Math Comput Sci.* 2015;25:53-63.
- [18]. Friedland. Treatment of bias in recursive filtering. *IEEE Trans Autom Contr.* 1969;AC-14(4):359-67.
- [19]. Kim KH, Lee JG, Park CG. Adaptive two-stage Kalman filter in the presence of unknown random bias. *Int J Adapt Control Signal Process.* 2006;20(7):305-19.
- [20]. Hsieh CS. Extension of unbiased minimum-variance input and state estimation for systems with unknown inputs. *Automatica.* 2009;45(9):2149-53.
- [21]. Gillijns S, Moor B. Unbiased minimum-variance input and state estimation for linear discrete-time systems. *Automatica.* 2007;43(1):111-16.
- [22]. Kitanidis PK. Unbiased minimum-variance linear state estimation. *Automatica.* 1987;23(6):775-78.
- [23]. Massoumnia MA. A geometric approach to the synthesis of failure detection filters. *IEEE Trans Automat Contr.* 1986;AC-31(9):839-46.
- [24]. White J, Speyer J. Detection filter design: Spectral theory and algorithms. *IEEE Trans Autom Control.* 1987;32:593-603.
- [25]. Hsieh S. Optimal minimum-variance filtering for systems with unknown inputs. *Proc World Congress on Intelligent Control and Automation (WCICA '06).* 2006 Jun;1:1870-74. Dalian, China.
- [26]. Saridis GN. *Self-Organizing Control of Stochastic Systems.* M. Dekker; 1977. (Control and Systems Theory; vol. 4). p. 488.
- [27]. Poliakov BT, Khlebnikov MV, Rapoport LB. *Mathematical Theory of Automatic Control: A Tutorial.* LENAND; 2019. ISBN 978-5-9710-6486-2. (in Russian). p. 500.
- [28]. Volovyk A, Kychak V, Havrilov D. Discrete Kalman Filter Invariant to Perturbations. *Acta Polytechnica Hungarica.* 2021;18(10):21-41. doi: 10.12700/APH.18.10.2021.10.2.
- [29]. Singer RA, Behnke KW. Real-Time Tracking Filter Evaluation and Selection for Tactical Applications. *IEEE Trans Aerosp Electron Syst.* 1971 Jan;AES-7(1):100-10. doi: 10.1109/TAES.1971.310257.
- [30]. Kychak VM, Volovyk YuM, Volovyk AY. *Methods and Devices for Processing Radio Signals of Airborne Landing Systems: Monograph.* VNTU; 2011. (in Ukrainian). p. 208.
- [31]. Mendel J. Computational requirements for a discrete Kalman filter. *IEEE Trans Automatic Control.* 1971 Dec;16(6):748-58. doi: 10.1109/TAC.1971.1099837.
- [32]. Voznesensky A, Butusov D, Rybin V, Kaplun D, Karimov T, Nepomuceno E. Denoising Chaotic Signals Using Ensemble Intrinsic Time-Scale Decomposition. *IEEE Access.* 2022;10:115767-75. doi: 10.1109/ACCESS.2022.3218052.
- [33]. Fekade B et al. Clustering hypervisors to minimize failures in mobile cloud computing. *Wireless Commun Mobile Comput.* 2016;16(18):3455-65. doi: 10.1002/wcm.2770.
- [34]. Klymash M et al. Spectral efficiency increasing of cognitive radio networks. In: *2013 12th International Conference: The Experience of Designing and Application of CAD Systems in Microelectronics, CADSM 2013;* 2013. Art. no. 6543226, p. 169-71.
- [35]. Maksymyuk T, Pelishok V. The LTE channel transmission rate increasing. In: *Proceedings of the 11th International Conference on Modern Problems of Radio Engineering, Telecommunications and Computer Science, TCSET'2012;* 2012. Art. no. 6192533, p. 251-52.